# *Ab-Initio* Studies of Alternant $X_2Y_2$ Rings (X = N, P, As, and Sb and Y = O, S, Se, and Te). Planar *versus* Butterfly Structures

**Jose M. Mercero, Xabier Lopez, Joseph E. Fowler, and Jesus M. Ugalde***

*Kimika Fakultatea, Euskal Herriko Unibertsitatea, P.K. 1072, 20080 Donostia, Euskadi, Spain*

*Received: February 17, 1997; In Final Form: May 14, 1997*[⊗]

Alternant $X_2Y_2$ (X = N, P, As, and Sb and, Y = O, S, Se, and Te) cyclic planar and butterfly like isomers have been studied at the complete-active-space self-consistent-field (CASSCF) molecular orbital and second-order configuration-interaction (SOCI) levels of theory with optimized basis sets including *f*-functions. The salient geometrical features, and trends in the intraanular X−X bond are discussed along with the relative energies between the isomers. Rationalization of the trends found in the relative energy is based on examining the various forms and magnitudes of bond strain present in each isomer.

## 1. Introduction

Four membered rings of the type $X_2Y_2$ formed with atoms of the group 15, X = N, P, As, and Sb, and group 16, Y = O, S, Se, and Te, have been recently recognized as the main building blocks of many chemical significant compounds. The $Te_2N_2$ ring can be identified as a part of larger tellurium dimide dimers[1] and $Sb_2O_2$ constitutes the central ring of many antimony containing molecules,[2] including $(SbPh_2O(Br)_2)_2$ whose structure has been solved recently.[3] Geothermal active sites,[4] where concentrations of arsenic and antimony are appreciable, are rich in sulfides of type $Sb_2S_2(SH)_2$, $Sb_2S_2(OH)_2$,[5] and $As_2S_2(OH)_2$[6] which are normally found solvated in water.

Also, since the stimulated emission pumping (SEP) experiments of Wodtke *et al.*[7] suggested the existence of high energy $N_2O_2$ isomers, these species have attracted renewed interest for their potential applications as new high energy density materials. However, the only isomer that has been characterized experimentally is the weakly bound *cis*-ONNO dimer.[8] $P_2O_2$ was detected as a combustion product of $P_2$ with $O_2$ in argon matrices, indicated by the ultraviolet photoexcitation of dipole-forbidden excited states of $P_2$.[9] For the $N_2S_2$ compound, the geometry has been determined by X-ray crystal structure analysis,[10,11] which shows that $N_2S_2$ is a very nearly square-planar ring with equivalent S−N bonds. Finally $Sb_2Te_2$ has also been detected in the gaseous phase over binary antimony/tellurium and tertiary antimony/tellurium/halogen alloys.[12]

However, in spite of the wealth of experimental information, there is still much to learn about the structural features of the four-membered rings present in all these species. In particular, their most interesting and controversial feature, namely whether they have a bipyramidal $C_{2v}$ symmetry (Figure 1a), with an intraanular X−X single bond, or a planar $D_{2h}$ symmetry (Figure 1b), with substantial biradical character on the group 15 X atoms, is still in debate. Indeed, the theoretical work available on these structures is very scarce and inconclusive.

Thus, while both $N_2O_2$[13] and $P_2O_2$[14−16] have been studied at an adequate level of theory to take into account the near degeneracy of the $b_{1u}$ and $b_{3g}$ molecular orbitals of the ring $\pi$ system, the $N_2S_2$[17,18] and $P_2S_2$[18] structures have only been studied by single reference methods, which are clearly insufficient to deal with these systems. Hence, we present in this paper, a study of both planar and butterfly-like $X_2Y_2$ (X = N, P, As, and Sb and Y = O, S, Se, and Te) singlet structures at a level of theory that deals correctly with the near-degeneracy effects and at the same time yields an accurate description of closed shell electronic configurations. The triplet states were not investigated as no butterfly structures with X−X bonds are possible for these states.

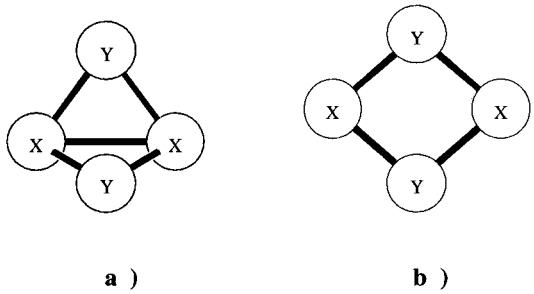


**Figure 1.** Butterfly (a) and planar (b) $X_2Y_2$ structures.

In order to sustain proper comparison between all the species considered, we have used relativistic effective core pseudopotentials (ECPs)[19] to build the basis sets for every atom. Notice that for the larger ones this is very convenient in order to design a workable representation of the chemically important valence electrons and to incorporate, through the ECPs, the effect of the relativistic contraction of the core atomic density.

This paper greatly broadens the expanse and applicability of theoretical studies on cyclic molecular structures formed by atoms of the groups 15 and 16. Through this work the underlying electronic structure which governs the geometrical structure of these systems is elucidated.

## 2. Methods

Geometries for all the species were fully optimized at the Hartree−Fock (HF) level of theory[20] and then reoptimized using the complete-active-space SCF CASSCF procedure.[21] Finally, to improve energies, we performed second-order configuration-interaction (SOCI)[22] single-point calculations using the CASSCF wave function as the reference wave function and the CASSCF-optimized geometry. Zero-point vibrational energy (ZPVE) corrections were obtained at the CASSCF level by a frequency calculation. The latter was used to confirm that all the structures were real minima, *i.e.*, they have all positive force constants.

The active space of the CASSCF wave function was carefully chosen and consists of two electrons in the X−X bonding and antibonding orbitals (see Figures 2 and 3). In the case of the butterfly structures, these two molecular orbitals were of $a_1$ and

[⊗] Abstract published in *Advance ACS Abstracts,* July 1, 1997.

S1089-5639(97)00585-9 CCC: $14.00 

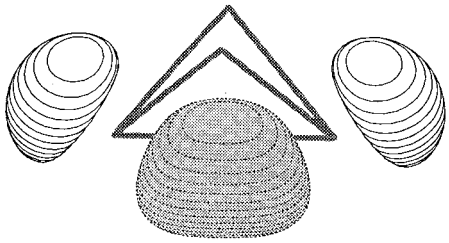

**a)** Orbital 11, $a_1$ symmetry.

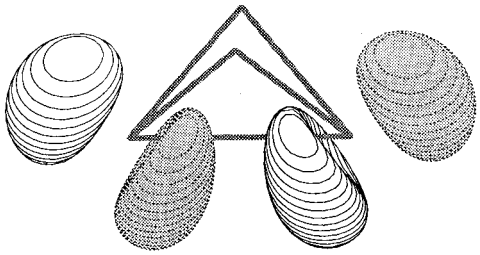

**b)** Orbital 12, $b_1$ symmetry.

**Figure 2.** The two orbitals included in the CASSCF(2,2) active space for the butterfly isomers. (a) The $\sigma_{xx}$ bonding orbital. (b) The antibonding $\sigma^*_{xx}$ orbital.

$b_1$ symmetry, while in the planar structures then $b_{1u}$ and $b_{3g}$ orbitals of the ring $\pi$ system were the ones included. It was confirmed further that this window size includes almost all of the nondynamical electron correlation. Indeed, the natural orbital occupancies of the external orbitals were less than 0.004 electrons in the subsequent SOCI wave function. (See Table 1 for the completed natural orbital occupancies at the SOCI/SKBJ+(d,f)//CASSCF(2,2)/SKBJ+(d).

The relativistic compact ECPs of Stevens *et al.*[23] (SKBJ) were used with their corresponding split valence basis set. This includes a 31 split valence contraction scheme for the first- and second-row atoms, and 41 scheme for the third and fourth row atoms. However, we augmented further these valence basis sets by adding a diffuse sp-set and a polarization d-set, resulting in a basis set that will be referred to hereafter as SKBJ+(d).

This basis set was used for the geometry optimization of every species considered in this paper. Notice that the geometries and energetics obtained with this basis set compare remarkably well with previous all ellectron basis set calculations of the smaller systems like $N_2O_2$,[13] $N_2S_2$,[17] $P_2O_2$,[14,16] and $P_2S_2$.[18] Nevertheless, in order to get even better relative energies, we improved our valence basis sets by adding one *f*-polarization set to the former SKBJ+(d) basis set. The exponents of both d and f-polarization functions of the resulting SKBJ+(d,f) basis set were energy optimized, at the MP2 level of theory, for their corresponding atoms. The final exponents are shown in Table 2. These two basis sets were used for the SOCI calculations, which generate 1953 configuration state functions (CFSs) using the smaller basis and 5253 CFS with the larger. All the calculations mentioned above were carried out with the GAMESS[24] suite of programs.

A topological analysis of the electron charge density[25,26] of the butterfly $P_2Y_2$, Y = O, S, and Se, isomers was also carried out. The aim of this was to shed light on the strength of the P−P bond with respect to the nature of the Y atom. Phosphorous compounds were taken as representative and conclusions were extended over the rest of the $X_2Y_2$ series. To achieve this goal, the HF/6-311+G(d) electron density was calculated with the GAUSSIAN94 suite of programs[27] and analyzed with the aid of the AIMPAC program.[28]

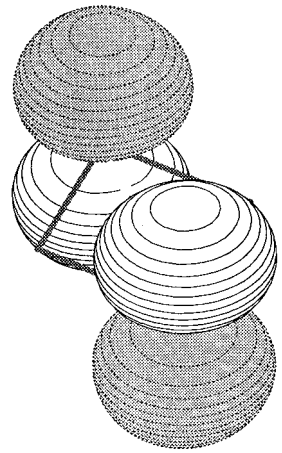

**a)** Orbital 11, $b_{1u}$ symmetry.

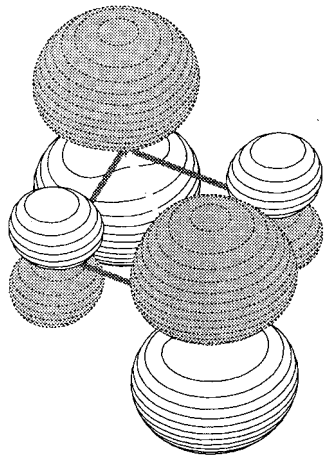

**b)** Orbital 12, $b_{3g}$ symmetry.

**Figure 3.** The two orbitals included in the CASSCF(2,2) active space for the planar isomers. (a) The molecular orbital of $b_{1u}$ symmetry. (b) The molecular orbital of $b_{3g}$ symmetry. Both orbitals have higher density on the X atom.

The MOLDEN, visualization of molecular and electronic structure, program[29] was used for the depiction of the molecular orbitals (see Figures 2 and 3).

## 3. Results

**3.1. $C_{2v}$ Symmetry Structures.** We have been able to optimize $C_{2v}$ symmetry (butterfly-like) structures for every combination of X and Y atoms, except for $N_2Y_2$, Y = Se and Te, which dissociate to $N_2$+ 2Y, at both the HF and the CASSCF(2,2) levels of theory due to the relative strengths of the N−N bond compared to the bonds of nitrogen with the large atoms. In the case of $Sb_2O_2$, the CASSCF(2,2) butterfly isomer converged to the planar isomer. Therefore, the MP2 method was used to optimize a butterfly structure for that system. The CASSCF(2,2) and SOCI results reported for that structure are single-point calculations performed at the MP2 geometry.

Table 3 collects the salient geometrical parameters of the butterfly structures found. Of special interest is the X−Y−X angle which increases with the size of X but decreases with larger Y atoms. There is generally a large difference in this angle between the Y = O and Y = S compounds, *e.g.*, 14.39° in the case of X = P. This large difference is due to the capacity of the larger atoms to more easily form acute bond angles.

**TABLE 1: Natural Orbital Occupancies of the CASSCF Active Space Orbitals, at the SOCI/SKBJ+(d,f) Level of Theory**

| | orbital 11, $a_1$ | orbital 12, $b_1$ | orbital 11, $b_{1u}$ | orbital 12, $b_{3g}$ |
|---|---|---|---|---|
| $N_2O_2$ | 1.94 | 0.05 | 1.76 | 0.23 |
| $N_2S_2$ | 1.95 | 0.04 | 1.93 | 0.06 |
| $N_2Se_2$ | | | 1.92 | 0.07 |
| $N_2Te_2$ | | | 1.67 | 0.32 |
| $P_2O_2$ | 1.91 | 0.08 | 1.66 | 0.33 |
| $P_2S_2$ | 1.95 | 0.04 | 1.78 | 0.21 |
| $P_2Se_2$ | 1.95 | 0.04 | 1.76 | 0.23 |
| $P_2Te_2$ | 1.96 | 0.03 | 1.74 | 0.26 |
| $As_2O_2$ | 1.85 | 0.14 | 1.57 | 0.42 |
| $As_2S_2$ | 1.92 | 0.06 | 1.70 | 0.29 |
| $As_2Se_2$ | 1.93 | 0.06 | 1.70 | 0.29 |
| $As_2Te_2$ | 1.94 | 0.05 | 1.69 | 0.31 |
| $Sb_2O_2$ | 1.87 | 0.11 | 1.47 | 0.52 |
| $Sb_2S_2$ | 1.91 | 0.08 | 1.63 | 0.37 |
| $Sb_2Se_2$ | 1.92 | 0.07 | 1.63 | 0.36 |
| $Sb_2Te_2$ | 1.93 | 0.06 | 1.64 | 0.35 |

**TABLE 2: Optimum *d*- and *f*-Exponents Used in the SKBJ+(d,f)**

| atom | *d* | *f* |
|---|---|---|
| oxygen | 1.053 251 | 1.263 742 |
| sulfur | 0.462 774 | 0.513 807 |
| selenium | 0.357 138 | 0.414 052 |
| tellurium | 0.250 786 | 0.319 116 |
| nitrogen | 0.780 742 | 0.984 663 |
| phosphorous | 0.363 807 | 0.412 786 |
| arsenic | 0.303 905 | 0.355 495 |
| antimony | 0.223 294 | 0.274 971 |

**TABLE 3: CASSCF(2,2) and HF (in Parenthesis) Geometries of Butterfly $X_2Y_2$ Species**

| species | X−X[a] | X−Y[a] | X−Y−X[a] | dihedral angle α[b] |
|---|---|---|---|---|
| $N_2O_2$ | 1.397 (1.337) | 1.407 (1.411) | 59.55 (56.56) | 109.68 (108.22) |
| $N_2S_2$ | 1.490 (1.389) | 1.747 (1.757) | 50.54 (46.55) | 113.13 (111.68) |
| $P_2O_2$ | 2.056 (2.001) | 1.696 (1.697) | 74.62 (72.26) | 113.76 (111.52) |
| $P_2S_2$ | 2.146 (2.102) | 2.139 (2.138) | 60.23 (58.88) | 109.17 (108.55) |
| $P_2Se_2$ | 2.176 (2.128) | 2.286 (2.286) | 56.85 (55.50) | 108.14 (107.89) |
| $P_2Te_2$ | 2.211 (2.158) | 2.515 (2.516) | 52.17 (50.79) | 107.55 (107.24) |
| $As_2O_2$ | 2.309 (2.222) | 1.822 (1.825) | 78.66 (74.99) | 115.59 (111.21) |
| $As_2S_2$ | 2.381 (2.324) | 2.272 (2.272) | 63.20 (61.54) | 108.86 (107.89) |
| $As_2Se_2$ | 2.408 (2.350) | 2.407 (2.407) | 60.04 (58.46) | 107.22 (107.22) |
| $As_2Te_2$ | 2.449 (2.387) | 2.625 (2.625) | 55.63 (54.08) | 107.18 (106.66) |
| $Sb_2O_2$[c] | 2.631 (2.572) | 2.103 (1.981) | 77.42 (80.94) | 111.68 (113.65) |
| $Sb_2S_2$ | 2.742 (2.676) | 2.460 (2.461) | 67.74 (65.87) | 109.46 (107.92) |
| $Sb_2Se_2$ | 2.767 (2.703) | 2.590 (2.591) | 64.55 (62.87) | 108.39 (107.21) |
| $Sb_2Te_2$ | 2.811 (2.815) | 2.814 (2.748) | 59.93 (58.42) | 107.07 (106.31) |

[a] Distances in angstroms. [b] Angles in degrees. [c] In the case of $Sb_2O_2$, MP2 and HF (in parenthesis) geometries are shown.

It is remarkable that the dihedral angle α is predicted to be fairly constant along the whole series, oscillating very mildly around the average value of 110°. Nevertheless, it is observed that α decreases slightly for each X in the $X_2Y_2$ series, with increasing the size of Y with the largest difference being a noticeable shrinking in α between Y = O and Y = S. The exception to this observation occurs with X = N. In this case, changing from Y = O to Y = S increases α by 3.5°.

Bond distances also show, some remarkable regularity patterns. Inspection of Figure 4, which charts the X−X and X−Y bond lengths, reveals that both X−X and X−Y bond lengths increase with a regular pattern. Note that both X−X and X−Y bond lengths are similar when X and Y belong to the same row and that the X−X bond length is larger than X−Y, when X belongs to a row that preceeds Ys row, and vice versa. Among all butterfly isomers, the largest X−X distance predicted by our calculations corresponds to the $Sb_2Te_2$ alternated ring, 2.811 Å and the shortest to $N_2O_2$, i.e., N−N = 1.397 Å.

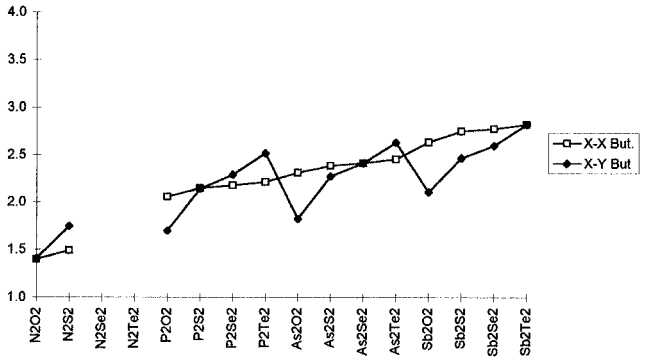


**Figure 4.** X−X and X−Y CASSCF(2,2) distances (in angstroms) in butterfly isomers as a function of the $X_2Y_2$ species.

**TABLE 4: CASSCF(2,2) and Hartree−Fock (in Parenthesis) Geometries of Planar $X_2Y_2$ Species**

| species | X−X[a] | Y−Y[a] | X−Y[a] | X−Y−X[b] |
|---|---|---|---|---|
| $N_2O_2$ | 1.924 (1.891) | 1.849 (1.820) | 1.334 (1.312) | 92.27 (92.20) |
| $N_2S_2$ | 2.277 (2.277) | 2.309 (2.305) | 1.621 (1.620) | 89.20 (89.31) |
| $N_2Se_2$ | 2.499 (2.447) | 2.576 (2.531) | 1.794 (1.760) | 88.27 (88.07) |
| $N_2Te_2$ | 2.732 (2.658) | 2.932 (2.863) | 2.004 (1.953) | 85.95 (85.76) |
| $P_2O_2$ | 2.473 (2.457) | 2.184 (2.162) | 1.650 (1.636) | 97.10 (97.30) |
| $P_2S_2$ | 3.011 (2.975) | 2.900 (2.865) | 2.090 (2.065) | 92.16 (92.14) |
| $P_2Se_2$ | 3.196 (3.152) | 3.113 (3.075) | 2.231 (2.202) | 91.50 (91.42) |
| $P_2Te_2$ | 3.521 (3.462) | 3.421 (3.374) | 2.455 (2.417) | 91.64 (91.48) |
| $As_2O_2$ | 2.693 (2.676) | 2.325 (2.292) | 1.779 (1.762) | 98.83 (98.84) |
| $As_2S_2$ | 3.191 (3.153) | 3.085 (3.034) | 2.219 (2.188) | 91.93 (92.19) |
| $As_2Se_2$ | 3.360 (3.314) | 3.289 (3.236) | 2.351 (2.316) | 91.22 (91.38) |
| $As_2Te_2$ | 3.686 (3.625) | 3.571 (3.514) | 2.566 (2.524) | 91.81 (91.77) |
| $Sb_2O_2$ | 3.002 (2.991) | 2.457 (2.423) | 1.940 (1.925) | 101.37 (101.97) |
| $Sb_2S_2$ | 3.490 (3.457) | 3.330 (3.269) | 2.412 (2.380) | 92.69 (93.22) |
| $Sb_2Se_2$ | 3.626 (3.558) | 3.555 (3.491) | 2.539 (2.503) | 91.14 (91.58) |
| $Sb_2Te_2$ | 3.942 (3.888) | 3.867 (3.799) | 2.761 (2.718) | 91.09 (91.33) |

[a] Distances in angstroms. [b] Angles in degrees.

In comparison with other theoretical works, our results are of very high quality. The N−N bond length of $N_2O_2$ (1.397 Å) agrees well with that obtained by Gordon *et al.*,[13] who reported a value of 1.395 Å at the CASSCF(10,10)/6-31G(d) level of theory. Notice that their active space, which contains the highest five bonding orbitals, is larger than ours. Nonetheless, their prediction is very close to ours, confirming further that all the important effects of the nondynamical electron correlation are well described by our (2,2) active space.

The N−N bond length of $N_2S_2$ butterfly isomer has also been reported earlier. Warren et al.[17] predicted a value of 1.394 Å at the MP2/6-31G* level of theory, which is notably shorter than our best value of 1.490 Å. This same trend holds also for the P−P bond length of both $P_2O_2$[16] and $P_2S_2$,[18] namely, earlier calculations at the MP2/6-31G* and HF/6-31G* levels of theory yield bond lengths of 2.032 and 2.097 Å, respectively, again shorter than our best predictions of 2.056 and 2.102 Å, respectively. Concomitantly, our predicted X−Y bond lengths are invariably slightly shorter values than earlier ab initio results. Compare 1.484 Å for N−O[13] with our best value of 1.397 Å, 1.761 Å for N−S[17] with our best value of 1.747 Å, 1.752 for P−O[16] with our estimation of 1.696 Å, and 2.136 for P−S[18] with our best value of 2.139. Finally, it is worth mentioning that all X−X and X−Y bond lengths discussed in this section are suggestive of single bonds.

**3.2. $D_{2h}$ Symmetry Structures.** The geometrical parameters of the $D_{2h}$ symmetry $X_2Y_2$ planar alternate rings are shown in Table 4. Comparison with their corresponding $C_{2v}$ symmetry butterfly like structures, collected in Table 3, shows a substantial lengthening of the X−X distance. Notice that in some cases this lengthening is greater than 1.0 Å, for example, for all the tellurium complexes and the $P_2Se_2$. This is indicative of the

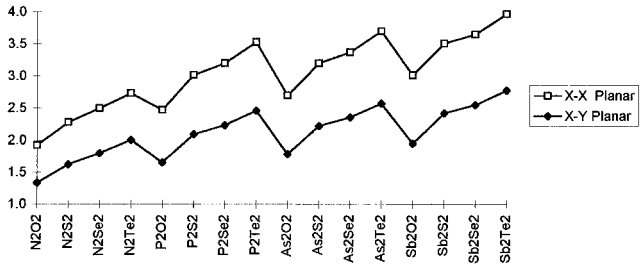


**Figure 5.** X−X and X−Y CASSCF(2,2) distances (in angstroms) in planar isomers as a function of the $X_2Y_2$ species.

fracture of the $\sigma_{xx}$ bond that has taken place for the planar isomers. However, the X−Y bond lengths of the planar isomers is still too long to suggest any double bond character in the X−Y bond.

As is expected from simple geometrical considerations, the planar isomers have significantly larger X−Y−X bond angles than their butterfly counterparts. This angle is rather invariant for X atoms larger than nitrogen and Y atoms larger than oxygen. There is a slight increase in this angle between the cases where X = N and those with larger X atoms. When Y = O, this angle increases steadily with increasing X size, reflecting oxygens resistance to angular bond strain. Also, there is a significant drop in the X−Y−X bond angle in moving from Y = O to Y = S, again reflecting the differences between the bonding tendencies of oxygen and the larger group 16 elements.

Figure 5 outlines the trend of the X−X distance and X−Y bond lengths along the $X_2Y_2$ series. Both distances follow the same pattern, which can be easily rationalized in terms of the van der Waals radii of the atoms.

In general, our geometries for planar structures agree reasonably with previous ab initio studies for $N_2O_2$[13] and $P_2O_2$.[14,16] The value of 1.970 Å for N−N and 1.365 Å N−O by Gordon *et al.*[13] lies within 0.05 Å of our results. The results computed at CASSCF(2,2)/6-31G* for planar $P_2O_2$[16] are very encouraging, since they show a remarkable agreement with our ECP's results (1.640 Å for P−O), indicating the excellent performance of relativistic effective core pseudopotentials throughout these complexes. Results for $N_2S_2$[17] and $P_2S_2$,[18] calculated at MP2/6-31G* level of theory, also show good agreement with our CASSCF results (N−S = 1.684 Å and P−S = 2.097 Å), and indicate (as remarked by Gordon et al.[13]) that MP2 leads to good geometries for these complexes despite the similar orbital energies of the $b_{1u}$ and $b_{3g}$ molecular orbitals.

There are a few experimental measurements for some of these species. In particular, both $P_2O_2$[9] and $S_2N_2$[10,11] have been isolated and $N_2Te_2$[1] and $Sb_2O_2$[2,3] have been detected as a part of bigger molecules. On the basis of X-ray crystallography data[10,11] a bond length between 1.651−1.657 Å was proposed for S−N bond of the planar $N_2S_2$ alternate ring, which differs only by 0.03 Å with respect to a our best value of 1.621 Å. A difference that should be attributed to both deficiencies in the calculation and the packing effects of the solid phase in which the experiments were carried out. X-ray crystallography data are also available for both $N_2T_{e2}$ and $Sb_2O_2$ planar alternate rings. However, due to their different chemical environment, both rings are slightly deformed, so that two different X−Y bond lengths are reported in each case. For the $Sb_2O_2$ entity,[3] the measured bond lengths are between 1.936 Å and 2.061 Å, which bracket narrowly our prediction of 1.940 Å. With respect to the N−Te bond length, our bond length of 2.004 Å agrees excellently with the experimental measurements of most of the known molecules containing this ring.[1] The available experimental evidence is in accordance with our work which supports predictions concerning the as-of-yet unobserved systems.

**TABLE 5: Relative Energies (kcal/mol) between Planar and Butterfly Structures**

| | $\Delta E$ (SKBJ+(d)) | | | $\Delta E$ (SKBJ+(d,f)) | | |
|---|---|---|---|---|---|---|
| species | HF[a] | CASSCF(2,2) | SOCI | HF | CASSCF(2,2) | SOCI |
| $N_2O_2$ | −17.02 | −34.87 | −33.46 | −16.64 | −33.98 | −31.92 |
| $N_2S_2$ | −37.37 | −27.92 | −28.28 | −37.89 | −29.2 | −29.30 |
| $P_2O_2$ | −5.60 | −21.77 | −20.00 | −3.19 | −20.03 | −17.26 |
| $P_2S_2$ | 11.76 | −0.13 | 1.78 | 13.87 | 2.69 | 5.30 |
| $P_2Se_2$ | 16.05 | 4.21 | 6.31 | 17.50 | 7.34 | 10.21 |
| $P_2Te_2$ | 17.21 | 5.17 | 7.56 | 19.11 | 8.23 | 11.50 |
| $As_2O_2$ | −4.65 | −20.47 | −19.00 | −3.97 | −19.83 | −17.76 |
| $As_2S_2$ | 12.10 | −0.11 | 1.69 | 12.17 | 0.84 | 3.28 |
| $As_2Se_2$ | 15.65 | 3.91 | 5.86 | 16.26 | 5.00 | 7.60 |
| $As_2Te_2$ | 17.89 | 5.89 | 8.06 | 17.36 | 6.71 | 9.55 |
| $Sb_2O_2$[b] | −7.47 | −37.58 | −35.68 | −4.61 | −39.05 | −36.16 |
| $Sb_2S_2$ | 10.80 | −2.43 | −0.75 | 11.25 | −1.25 | 1.16 |
| $Sb_2Se_2$ | 14.00 | 1.69 | 3.46 | 15.09 | 3.09 | 5.58 |
| $Sb_2Te_2$ | 17.01 | 5.51 | 7.43 | 17.61 | 6.69 | 9.33 |

[a] HF = Hartree Fock. [b] For $Sb_2O$ butterfly isomer, CASSCF(2,2) and SOCI single-point energies over MP2-optimized geometry was employed.

**3.3. Relative Energies.** Relative energies between butterfly and planar structures ($\Delta E_{p-b}$) at HF, CASSCF(2,2), and SOCI levels of theory and with two basis sets (one without *f*-functions and the other one including them) are shown in Table 5.

Notice that the inclusion of the main part of the nondynamic correlation, through CASSCF(2,2) level of theory, leads to a significant stabilization of the planar ring, due to the appropriate handling of the biradical character of these cycles. This stabilization is quite significant, around 10−16 kcal/mol. Indeed, it is known that the CASSCF methods exaggerate the stability of biradical like structures.[30] This overestimation is corrected by the SOCI calculations, which, as shown in Table 5, reduce the stabilization energy of the CASSCF with respect HF for the planar structures by approximately 2 kcal/mol. Notice that inclusion of *f*-functions also favor the butterfly species by a similar amount of energy (2 kcal/mol). At our best level of theory [SOCI/SKBJ+(d,f)//CAS(2,2)/SKBJ+(d)] only the $N_2S_2$ and all the oxygen-containing planar structures are found to be more stable than their corresponding butterfly like ones.

All oxygen-containing planar species are more stable than their corresponding butterfly species. The largest energy difference between the planar and butterfly-like isomers is found for the $N_2O_2$ species, namely −31.92 kcal/mol. Quite curiously, all attempts to detect this compound experimentally have failed up to date.[7] Earlier *ab initio* calculations[13] at the PT2F/6-311+G(2d,f)//CASSCF(10,10)/6-31G(d) level of theory gave a relative energy between the planar and butterfly-like structures of −28.7 kcal/mol.

The substitution of nitrogen by phosphorus, arsenic, or antimonium leads to lower figures for the stabilization energy, around −17 kcal/mol. *Ab-initio* data for $P_2O_2$ system is also available. Mühlhaüser *et al.*[16] performed very accurate *ab initio* calculations of $\Delta E_{p-b}$ for the $P_2O_2$ species. They report a value of −20.5 kcal/mol at the MRD-CI level of theory which raises up to −25.9 kcal/mol when they include size consistency corrections. Our SOCI results are close to the MRD-CI value, especially if we consider that their basis set does not include *f*-functions and so, their data should be compared with our SOCI/SKBJ+(d) value, i.e., −20.0 kcal/mol. To the best of our knowledge, there are not previous calculations for $As_2O_2$ and $Sb_2O_2$. Our data suggest that their relative energies are close to that of $P_2O_2$, and hence, planar isomers are expected to be favored in both cases.

Substituting oxygen by sulfur stabilizes butterfly isomers with respect to the planar cyclic structures. At our highest level of

theory, only planar $N_2S_2$ lies energetically below its corresponding butterfly-like isomer, i.e., −29.31 kcal/mol. The stability of this planar ring was also claimed by other authors. Warren *et al*.[17] reported this structure as a global minimum of the $N_2S_2$ PES, with a relative energy between 35−45 kcal/mol respect to the butterfly isomer. Recall that planar $N_2S_2$ and $P_2O_2$ are the only species isolated experimentally up to now.

On the other hand, the butterfly structures of $P_2S_2$, $As_2S_2$, and $Sb_2S_2$ are more stable than planar ones. For the $P_2S_2$ isomer, we obtain the fact that the butterfly isomer is 5.30 kcal/mol more stable than the planar at the SOCI/SKBJ+(d,f)//CASSCF(2,2)/SKBJ+(d) level of theory. The isomeric energy differences of 3.28 and 1.16 kcal/mol for $As_2S_2$ and $Sb_2S_2$ are too small to be conclusive, and we cannot rule out that higher levels of theory would change their stability order.

Finally, in the case of the selenium and tellurium systems (except for nitrogen compounds where butterfly isomers were not found as stationary points of the PES), butterfly structures are clearly more stable than planar isomers. These compounds have the largest relative stabilities of the butterfly structures with respect to the planar structures.

Considering the above-mentioned tendencies, it is noted that larger Y atoms leads to an overall stabilization of the butterfly isomers. This effect is most pronounced when we go from first-row atoms to second-row ones, i.e., substituting oxygen by sulphur. In the next section we try to shed light on this behavior, providing simple, effective models for comprehension of these trends.

## 4. Discussion

In spite of the lack of an X−X bond in the planar ring, our results show that for oxygen and nitrogen containing cyclic species, this conformation is preferred over the butterfly one. At a first glance, this may be surprising. It can be expected that isomers with some biradical character will stabilize upon evolving to isomers in which all electrons are included in bonding, as we observed for third- and fourth-row atoms containing complexes in this study. In our $X_2Y_2$ compounds, in order to form the X−X bond, the X atoms must pyramidalize. However, this pyramidalization shrinks the X−Y−X angle which, in turn, causes additional bond angle strain at the Y atom, destabilizing the system. It is the interplay and the magnitude of these important factors which determine which of the two isomers will be more stable.

First, let us consider the increase of angular bond strain at the Y atoms in going from the planar to the butterfly structures. We note that there are severe differences in the X−Y−X angle between the two structures. Using the $P_2Y_2$ series as an example, we find differences of 22.48° for $P_2O_2$, 31.93° for $P_2S_2$, 34.65° for $P_2Se_2$, and 39.47° for $P_2Te_2$.

Oxygen atoms are particularly resistant to forming acute bond angles. It has been seen throughout this work that in both the planar and butterfly isomers the X−Y−X is largest when Y = O. It is because of oxygen's inability to efficiently form small bond angles that all of the $X_2O_2$ planar isomers are more stable than their butterfly counterparts. For these systems, the loss of energy due to angular bond strain at the Y atom is greater than the energy gained by forming the X−X bond. Larger Y atoms are more capable of forming acute bond angles. Thus, the energy lost in shrinking these X−Y−X angles is less than in the Y = O complexes and here the stabilization gained from forming the X−X bond outweighs this loss.

Additionally, we note that the X−X bonds of the butterfly structures are also strained. The bond angles of the tricoordinated X atoms are far from the optimal values. The strain on the X−X bond is indicated by the form of the $\sigma_{xx}$ orbital depicted the Figure 2a. Notice that the probability density is concentrated outside of the line connecting the two X atoms.

This nonoptimum pyramidalization was not the same for all the complexes. In Table 3 we show the dihedral angles for butterfly structures, indicating the degree of pyramidalization of the X atoms, smaller angles reflecting bond angles closer to the optimal. This angle decreases with larger Y atoms and the greatest decrease occurs between oxygen and sulfur. Therefore, it is clear that the smaller Y atoms (especially oxygen) yield smaller pyramidalizations, hence, less stable butterfly structures.

To further confirm this point, we carried out a Bader analysis on the following series: $P_2O_2$, $P_2S_2$, and $P_2Se_2$ with the HF/6-311+G(d) wave function. The Bader analysis provides a direct measure of the strain of a bond by means of the difference between the geometrical and bond path lengths. The largest bond strain was obtained for the P−P bond of the $P_2O_2$ complex, namely 0.1607 a.u. This bond strain was substantially lowered for $P_2S_2$ and $P_2Se_2$: 0.0680 and 0.0553 au, respectively.

Summarizing, one can conclude that while butterfly structures should be stabilized over planar ones due to bonding arguments, the strain on the X−Y−X angle leads to a destabilization of these structures. Additionally, for the complexes with small Y atoms the X−X bond is significantly strained and therefore the stabilization gained by forming that bond is reduced. These destabilization factors are particularly important for oxygen containing compounds. Indeed, planar isomers are favored in these molecules. When the various bond strains are reduced with larger Y atoms, the energy gained from bond formation outweighs the energy lost due to bond strain and the butterfly isomer is favored.

## 5. Conclusions

We have performed high-level ab-initio calculations (HF, CASSCF(2,2), and SOCI) with basis sets containing *f*-functions for a series of butterfly and planar $X_2Y_2$ species, where X = N, P, As, and Sb and Y = O, S, Se, and Te. From our study we can draw the following conclusions. 1. Both planar and butterfly $X_2Y_2$ correspond to stable isomers of the corresponding PESs, excluding $N_2Se_2$ and $N_2Te_2$ (additionally, the existence of butterfly $Sb_2O_2$ cannot be definitely stated as no such structure was found with the CASSCF(2,2) method). 2. The main atomic distance differences between butterfly and planar isomers are an elongation of the X−X distance (due to the fracture of the X−X bond) and a slight shrinking of the X−Y bond lengths. 3. The planar−butterfly relative energies show similar tendencies for phosphorus, arsenic, and antimony. Planar isomers are favored over butterfly ones for oxygen-containing species. For sulfur-containing species similar energetics are obtained, and for selenium and tellurium butterfly-like structures are clearly more stable. 4. The angular bond strain at the Y atoms and the weakening of the X−X bond due again to bond strain reduce the stability of the butterfly isomers. With the larger Y atoms, these factors are greatly reduced leading to a preference for the butterfly isomer. 5. Both nitrogen complexes favor planar structures. Recall that large Y atom (Y = Se and Te) nitrogen butterfly isomers dissociate to $N_2$ + 2Y (Y = Se and Te).

## 6. Acknowledgment

This research has been supported by the University of the Basque Country (Euskal Herriko Unibertsitatea) and the Basque Government (Eusko Jaurlaritza), Grant GV/203.215-49/94. J.M.M. and J.E.F. wish to thank the Basque Government (Eusko Jaurlaritza) for a grant.

## References and Notes

(1) Chivers, T.; Gao, X.; Parvez, M. *Inorg. Chem.* **1996**, *35*, 9. Chivers, T.; Gao, X.; Parvez, M. *Inorg. Chem.* **1996**, *35*, 4336.
(2) Bordner, J.; Doak, G. O.; Everett, T. S. *J. Am. Chem. Soc.* **1986**, *108*, 4206.
(3) Southerington, I. G.; Forster, G. E.; Begley, M. J.; Sowerby, D. B. *J. Chem. Soc., Dalton Trans.* **1995**, *12*, 1995.
(4) White, D. E. *Econ. Geol.* **1981**, *75*, 392 (Anniversary Volume).
(5) Krupp, R. E. *Geochim. Cosmochim. Acta* **1988**, *52*, 3005.
(6) Krupp, R. E. *Geochim. Cosmochim. Acta* **1990**, *54*, 3239.
(7) Yang, X.; Kim, E. H.; Wodtke, A. M. *J. Chem. Phys.* **1992**, *96*, 5111. Yang, X.; Price, J. M.; Mack, J. A.; Morgan, C. G.; Rogaski, C. C.; McGuire, D.; Kim, E. H.; Wodtke, A. M. *J. Chem. Phys.* **1993**, *97*, 3944.
(8) Fischer, I.; Strobel, A.; Staecker, J.; Niedner-Schatteburgh, G.; Muller-Dethlefs, K.; Bondybey, V. E. *J. Chem. Phys.* **1992**, *96*, 7171.
(9) Mielke, Z.; MacCluskey, M.; Andrews, L. *Chem. Phys. Lett.* **1990**, *165*, 146. MacCluskey, M.; Andrews, L. *J. Phys. Chem.* **1991**, *95*, 2679.
(10) Mikulski, C. M.; Russo, P. J.; Saran, M. S.; MacDiarmid, A. G.; Garito, A. F.; Heeger, A. J. *J. Am. Chem. Soc.* **1975**, *97*, 6358.
(11) Cohen, M. J.; Garito, A. F.; Heeger, A. J.; MacDiarmid, A. G.; Mikulski, C. M.; Saran, M. S.; Kleppinger, J. *J. Am. Chem. Soc.* **1976**, *98*, 3844.
(12) Poth, L. and Weil, G. *J. Phys. Chem.* **1995**, *99*, 551.
(13) Nguyen, K. A.; Gordon, M. S.; Montgomery, J. A., Jr.; Michels, H. H. *J. Phys. Chem.* **1994**, *98*, 10072.
(14) Lopez, X.; Sarasola, C.; Lecea, B.; Largo, A.; Barrientos, C.; Ugalde, J. M. *J. Phys. Chem.* **1993**, *97*, 4078.
(15) Bruna, P. J.; Mühlhaüser, M.; Peyerimhoff, S. D. *Chem. Phys. Lett.* **1991**, *180*, 606.
(16) Mühlhaüser, M.; Engels, B.; Ernzerhof, M.; Marian, C. M.; Peyerimhoff, S. D. *J. Phys. Chem.* **1996**, *100*, 120.
(17) Warren, D. S.; Zhao, M.; Gimarc, M. *J. Am. Chem. Soc.* **1995**, *117*, 10345.
(18) Janssen, R. A. J. *J. Phys. Chem.* **1993**, *97*, 6384.
(19) Goddard W. A., III *Phys. Rev. A* **1968**, *174*, 659. Melius, C. F.; Goddard W. A., III *Phys. Rev. A* **1974**, *10*, 1528. Kahn, L. R.; Baybut, P.; Truhlar, J. *J. Chem. Phys.* **1976**, *75*, 3826.
(20) For complete description of the basis sets and the methods used, see: Hehre, W. J.; Random, L.; Schleyer, P. v. R.; Pople, J. A. *Ab initio Molecular Orbital Theory*; Wiley: New York, 1986; pp 63−100.
(21) Lengsfield, B. H., III *J. Chem. Phys.* **1980**, *73*, 328. Jarkony, D. R. *Chem. Phys. Lett.* **1981**, *77*, 634. Ruedenberg, K.; Schmidt, M. W.; Dombeck, M. M.; Elbert, S. T. *Chem. Phys.* **1982**, *71*, 41, 51, 65. Lam, B.; Schmidt, M. W.; Ruedenberg, K. *J. Phys. Chem.* **1985**, *89*, 2221.
(22) Schmidt, M. W.; Truong, P. N.; Gordon, M. S. *J. Am. Chem. Soc.* **1987**, *109*, 5217.
(23) Stevens, W. J.; Krauss, M.; Basch, H.; Jasien, P. G. *Can. J. Chem.* **1992**, *70*, 612.
(24) For GAMESS (General Atomic and Molecular Electronic Structure System) example references, see: (a) Schmidt, M. W.; Baldridge, K. K.; Boatz, J. A.; Jensen, J. H.; Koseki, S.; Gordon, M. S.; Nguyen, K. A.; Windus, T. L.; Elbert, S. T. *QCPE Bull.* **1990**, *10*, 52. (b) Schmidt, M. W.; Baldridge, K. K.; Boatz, J. A.; Elbert, S. T.; Gordon, M. S.; Jensen, J. H.; Koseki, S.; Matsunaga, N.; Nguyen, K. A.; Su, S.; Windus, T. L. *J. Comput. Chem.* **1993**, *14*, 1347.
(25) Bader, R. F. W. *Atoms in Molecules. A Quantum Theory*; Oxford Science Publications: Oxford, 1990; Chapter 7.
(26) Boyd, R. J.; Ugalde, J. M. In *Computational Chemistry Part A*; Fraga, S., Ed.; Elsevier: Amsterdam, 1992.
(27) Frisch, M. J.; Trucks, G. W.; Schlegel, H. B.; Gill, P. M. W.; Johnson, B. G.; Robb, M. A.; Cheesemen, J. R.; Keith, T. A.; Petersson, G. A., Montgomery, J. A.; Raghavachari, K.; Al-Laham, M. A.; Zakrzewski, V. G.; Ortiz, J. V.; Foresman, J. B.; Ciolowski, J.; Stefanov, B.; Nanayakkara, A.; Challacombe, M.; Peng, C. Y.; Ayala, P. Y.; Chen, W.; Wong, M. W.; Andres, J. L.; Replogle, E. S.; Gomperts, R.; Martin, R. L.; Fox, D. J.; Binkley, J. S.; Defrees, D. J.; Baker, J.; Stewart, J. P.; Head-Gordon, M.; Gonzalez, C.; Pople, J. A. *GAUSSIAN 94*, Revision B.1 Pittsburgh, PA, 1995.
(28) Biegler-Koning, F. W.; Bader, R. F. W.; Tang, T. H. *J. Comput. Chem.* **1980**, *27*, 1924.
(29) For the MOLDEN program, see: http://www.caos.kun.nl/∼schaft/molden/molden.html
(30) Kozlowski, P. M.; Dupuis, M.; Davidson, E. R. *J. Am. Chem. Soc.* **1995**, *117*, 774. Borden, W. T.; Davidson, E. R. *Acc. Chem. Res.* **1996**, *29*, 67.